Prospects for cooling and trapping rotationally hot molecules

R. C. Forrey
Penn State University, Berks-Lehigh Valley College, Reading, Pennsylvania 19610-6009
(Received 20 March 2002; published 27 August 2002)

Cold collisions involving highly rotationally excited diatomic molecules are investigated. As the translational energy is lowered, the total inelastic cross section decreases sharply for specific channels where quasiresonant transitions are no longer energetically allowed. Rate coefficients are given for collisional quenching of rotationally excited H_2, D_2, T_2, and O_2 at zero temperature. The specific rotational states that are stable against collisional relaxation would be interesting prospects for cooling and trapping. The application of collisional cooling methods together with recently developed schemes for producing rotationally hot molecules may allow high densities of ultracold "super rotors" to be achieved.

DOI: 10.1103/PhysRevA.66.023411 PACS number(s): 33.80.Ps

I. INTRODUCTION

Experimental schemes to produce diatomic molecules in highly excited rotational states have been proposed [1,2] and recently realized [3]. The results of these experiments may have important implications for both gas phase and surface physics and chemistry [3].

Theoretical calculations have revealed interesting behavior for the collisional dynamics of such rotationally hot molecules at low temperatures [4–7]. One intriguing result of the calculations [6] is the possibility for producing rotationally hot molecules that are stable against collisional relaxation. The idea is to use molecular levels that would undergo a quasiresonant (QR) vibration-rotation (VR) transition at normal temperatures. At very low temperatures, the highly efficient and specific QRVR transition may become closed due to energy conservation. This effectively stabilizes the rotationally hot molecule against collisional deexcitation [6]. For molecules that are also vibrationally excited, the rotational distribution of total quenching rate coefficients is nearly symmetric about the levels where QRVR transitions are energetically closed [4]. This is due to highly efficient energy transfer that allows vibrational excitation and deexcitation to occur with nearly equal probability. Observations from the optical centrifuge experiments [3] have suggested that at least some of the highly rotating molecules are produced without vibrational excitation. For collisions that involve molecules in the vibrational ground state, the rotational distribution of total quenching rate coefficients is asymmetric with respect to levels where QRVR transitions are closed because the molecules cannot lose vibrational energy. In this work, we provide an extensive account of the rotational distributions for collisional quenching of the lowest-lying vibrational levels for several types of rotationally excited molecules.

The collision partner in each calculation is a helium atom, however, the characteristic behavior in the distribution of rate coefficients applies to any weakly interacting system. For example, when helium is replaced by argon, the shape of the rotational distributions for the lowest-lying vibrational quenching rate coefficients at zero temperature is unchanged [8]. Other rare-gas collision partners have been used in QRVR transfer experiments at ordinary temperatures [9]. The choice of helium as a collision partner at low temperatures is a natural one considering the experimental progress in helium buffer gas cooling [10] and helium cluster isolation spectroscopy [11]. Because some of the rotationally hot molecules are stable against collision with other atoms and molecules, it is very possible that they would also be stable upon collision with a surface, such as a helium coated wall or droplet. If the sticking probability is large, then the so-called "super rotors" would be trapped by the surface for many rotational periods. An analogy with molecular predissociation suggests that the molecules could be trapped in this manner for several milliseconds or more before being lost to relaxation [5]. If the sticking probability is low, as in the Wigner threshold regime where it approaches zero, then it may also be possible to use the surfaces as a means for containing the highly rotating molecules.

It has been speculated [6,7] that the quasiresonant effect should be most pronounced for light diatomic systems due to the small moment of inertia. Investigation of helium collisions with hydrogen, deuterium, and tritium molecules should provide insight into the importance of the moment of inertia in quasiresonance phenomena. We show the results of this investigation, and based on these results, we draw conclusions for other systems such as Li_2 and O_2. The dependence of the total inelastic cross section on the anisotropy of the potential-energy surface is also studied. We find that light diatomic systems with small long-range anisotropy generally allow very stable rotationally excited states when the QRVR channels are closed. This is primarily due to the exponential decay of the rate coefficients for pure rotational transitions as the energy gap between the initial and final state is increased [12,13]. Heavier systems with large long-range anisotropy have rate coefficients for pure rotational transitions that fall off more slowly with energy gap allowing more efficient relaxation even when QRVR transitions are closed.

The paper is organized as follows: Section II briefly describes the classical theory of quasiresonant scattering along with a general description for estimating the collisional quenching behavior of any highly rotating diatomic system. The usual quantum-mechanical formulation is reviewed together with the scattering length description for inelastic collisions in the limit of zero temperature. Section III presents the results of the quantum calculations for several systems

 ©2002 The American Physical Society

and provides an interpretation based on the theory developed in Sec. II. Conclusions and speculations for future work are given in Sec. IV.

II. THEORY

It is well known [12,13] that rotational quenching decreases rapidly with the energy gap between initial and final diatomic states. As the rotational level of the molecule increases, the energy gap for pure rotational transitions also increases, and the efficiency decreases. Therefore, QRVR may be the dominant energy-transfer mechanism at very high rotational levels. Several classical studies of QRVR energy transfer have been reported [7,14–16] for atom-diatom collisions at ordinary temperatures. It has also been shown [4,5] that collisional quenching rate coefficients are strongly influenced by classical dynamics in the $T\rightarrow 0$ limit. If v and j are the vibrational and rotational quantum numbers of the diatom, then the general rule followed by QRVR transitions is

$$\Delta I = n_j \Delta j + n_v \Delta v = 0, \tag{1}$$

where $I = n_j j + n_v v$ is the conserved action and n_j and n_v are small integers. When the vibrational and rotational motion are in approximate low-order resonance, the condition

$$n \equiv n_v / n_j \approx \omega_v / \omega_j, \tag{2}$$

also holds, where ω_v and ω_j are the classical vibrational and rotational frequencies of the diatom. If n is an even integer for homonuclear diatoms, then an integral number of complete vibrations will occur during each half rotation and essentially all of the classical trajectories will obey the quasiresonant rule (1) for a single (n_v, n_j) pair [14]. This produces a correlation between Δv and Δj that persists all the way down to zero temperature [4,5]. If the QRVR transition is energetically allowed, this correlation takes the form of a propensity rule [14]

$$\Delta j = -n \Delta v. \tag{3}$$

Equations (1) and (2) may be used to show that

$$\Delta E_{\text{int}} = \frac{\partial H}{\partial v} \Delta v + \frac{\partial H}{\partial j} \Delta j = \hbar \omega_v \Delta v + \hbar \omega_j \Delta j \approx 0, \tag{4}$$

which is the condition that the internal energy change during the collision is as small as possible. As the translational energy approaches zero, the classical dynamics continues to satisfy Eqs. (3) and (4) by allowing Δv and Δj to be much smaller than a single quantum. This means that the classical analog of the quantum process is forbidden. Nevertheless, it has been shown [4,5] that the quantum process is strongly influenced by the classical dynamics when the initial rotational level is near a quasiresonant value $j_{QR}^{(n)}$ for integer n.

One of the interesting features of ultracold atom-diatom collisions is the efficiency and specificity of the QRVR transitions for a range of j values centered at $j_{QR}^{(n)}$. For a molecule that is oscillating harmonically with frequency ω_e, the nth-order QR rotational level is

TABLE I. Harmonic approximation.

Molecule	ω_e(cm^{-1})	B_e(cm^{-1})	D_e(cm^{-1})	j_D	$j_{QR}^{(2)}$	$j_{QR}^{(4)}$
H_2	4401.2	60.85	38292.5	25	18	9
Li_2	351.43	0.6726	8517	113	130	65
O_2	1580.2	1.446	42050.2	171	273	137

$$j_{QR}^{(n)} = \frac{\omega_e}{2nB_e}, \tag{5}$$

where the rotational constant B_e is inversely related to twice the moment of inertia of the molecule. In the zero-temperature limit, the nth-order transition is typically closed for $j = j_{QR}^{(n)}$ while the neighboring j values allow very efficient QRVR energy transfer [4]. The largest rotational level with an energetically closed QRVR transition occurs when $n=2$. Because the efficiency of pure rotational quenching decreases rapidly with increasing j, the $j = j_{QR}^{(2)}$ rotational levels have the best chance to resist collisional relaxation. In order to produce highly rotationally excited molecules that are stable against collisional decay, it is usually necessary that the QR rotational level be less than the dissociation rotational level

$$j_D = \sqrt{\frac{D_e}{B_e}}, \tag{6}$$

where D_e is the dissociation energy. Table I shows the harmonic parameters and also the rotational quantum numbers for hydrogen, lithium, and oxygen molecules. It is apparent from the table that the second-order QR rotational levels for Li_2 and O_2 occur at values that are greater than the levels for dissociation. Therefore, there is very efficient vibrational and rotational energy exchange for the highly excited states of these molecules. Figures 1–3 show results that go beyond the harmonic approximation for all three of these molecules. The energy gaps were computed using the potential curve of

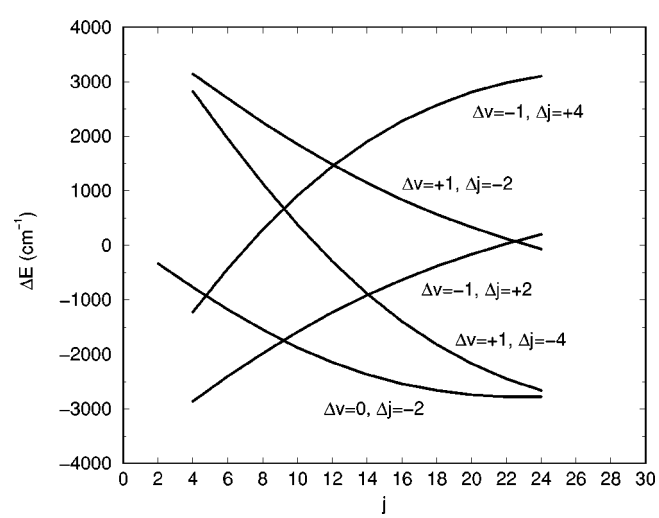

FIG. 1. Internal energy change versus j for collisions involving the ground $X^1\Sigma_g^+$ state of $H_2(v=1,j)$.

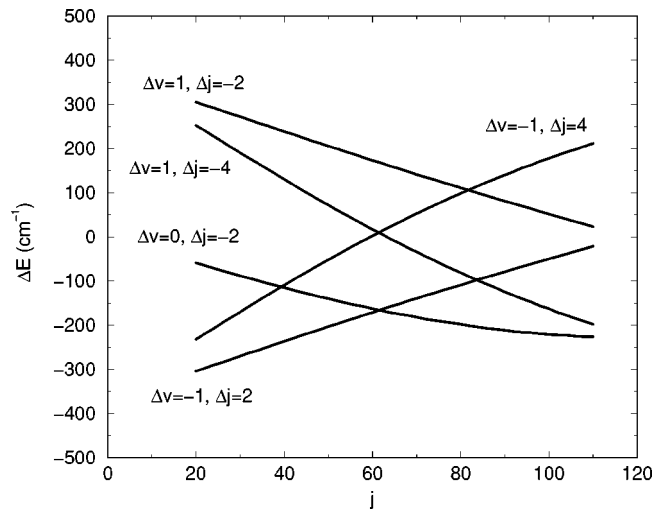

FIG. 2. Internal energy change versus j for collisions involving the ground $X^1\Sigma_g^+$ state of $^6Li_2(v=1,j)$.

Schwenke [17] for H_2, Zemke and Stwalley [18] for Li_2, and Friedman [19] for O_2 (as modified by Babb and Dalgarno [20]). The internal energy change is plotted versus j for H_2, Li_2, and O_2 molecules each in the $v=1$ initial state. In each figure, the increasing curves correspond to $\Delta j>0$ transitions and the decreasing curves to $\Delta j<0$ transitions. When the internal energy change is positive, the transition is not allowed for $T\rightarrow 0$ due to energy conservation. Interesting behavior will generally be found near j values where the increasing and decreasing curves intersect for a given $\Delta j=-n\Delta v$ transition. This intersection point may be used to define $j_{QR}^{(n)}$, replacing the approximate value given in Eq. (5). If the curves intersect at a positive value, then there will be a sharp decrease in the total inelastic deexcitation rate coefficient. The most pronounced behavior will occur for $n=2$ because the pure rotational quenching contribution is also very small. For H_2 molecules, the $n=2$ case occurs at $j=22$ which is less than the j value for dissociation. It is these molecules that are most stable against collisional relaxation

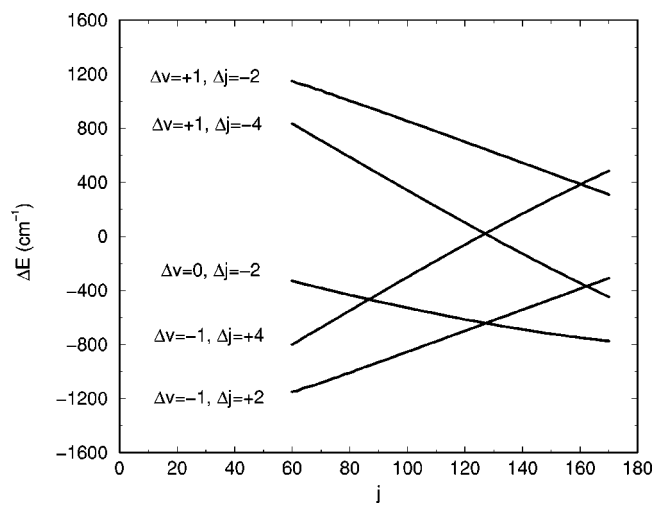

FIG. 3. Internal energy change versus j for collisions involving the ground $X^3\Sigma_g^-$ state of $O_2(v=1,j)$.

[6]. The vibrational ground state may allow a range of j values that are less than $j_{QR}^{(2)}$ to be stable against collision even when $j_{QR}^{(2)}$ is greater than j_D. This is due to the removal of the quasiresonant $\Delta v=-1$ transition. Because the $j_{QR}^{(2)}$ values are greater than the j_D values for Li_2 and O_2 molecules, there is no chance for bound vibrationally excited states of these molecules to be stable against collision. However, it may be possible for quasibound states with $v>0$ to be stable if the dissociation lifetime is large enough [21]. For example, the lithium molecule has many quasibound levels whose tunneling widths for $j<130$ are small enough that dissociation cannot occur on any reasonable time scale [2]. Extrapolation of the $\Delta j=-2\Delta v$ curves of Fig. 2 shows that there should be a positive energy-gap crossing in the vicinity of $j=120$. Therefore, the lithium molecule may possess a quasibound state whose stability against collision is limited only by the rate coefficient for pure rotational quenching.

In the following section, we present results of numerically converged quantum-mechanical calculations. The formulas are summarized below. The rate coefficients are given by

$$R_{vj\rightarrow v'j'}(T)=(8k_BT/\pi\mu)^{1/2}\frac{1}{(k_BT)^2}\int_0^\infty \sigma_{vj\rightarrow v'j'} \times \exp(-E_{vj}/k_BT)E_{vj}dE_{vj}, \tag{7}$$

where T is the temperature, k_B is the Boltzmann constant, μ is the three-body reduced mass, and E_{vj} is the translational energy in the incoming channel. The energy-dependent cross section is given by

$$\sigma_{vj\rightarrow v'j'}=\frac{\pi}{2\mu E_{vj}(2j+1)}\sum_{J=0}^{\infty}(2J+1)\sum_{l=|J-j|}^{|J+j|}\sum_{l'=|J-j'|}^{|J+j'|} \times|\delta_{jj'}\delta_{ll'}\delta_{vv'}-S^J_{jj'll'vv'}|^2, \tag{8}$$

where l is the orbital angular momentum and $\vec{J}=\vec{j}+\vec{l}$ is the total angular momentum. The scattering matrix S is obtained from the solution of the usual close-coupling equations [22]. In the zero-temperature limit, the thermal average in Eq. (7) simplifies and the rate coefficient is simply the cross-section times the collision velocity. The total collisional quenching (or relaxation) rate coefficient for a given v and j level is given by the sum of $R_{vj\rightarrow v'j'}$ over all possible values of v' and j'. Equations (7) and (8) may be used to obtain the components of the complex scattering length $a_{vj}=\alpha_{vj}-i\beta_{vj}$. The imaginary part is determined by

$$\lim_{T\rightarrow 0}R_{vj}(T)=\frac{4\pi\hbar\beta_{vj}}{\mu}, \tag{9}$$

and the real part by

$$\sigma_{vj\rightarrow vj}=4\pi(\alpha_{vj}^2+\beta_{vj}^2), \tag{10}$$

which is the elastic-scattering cross section in the limit of zero energy. The cross sections are generally very sensitive to the details of the potential-energy surface. It was shown

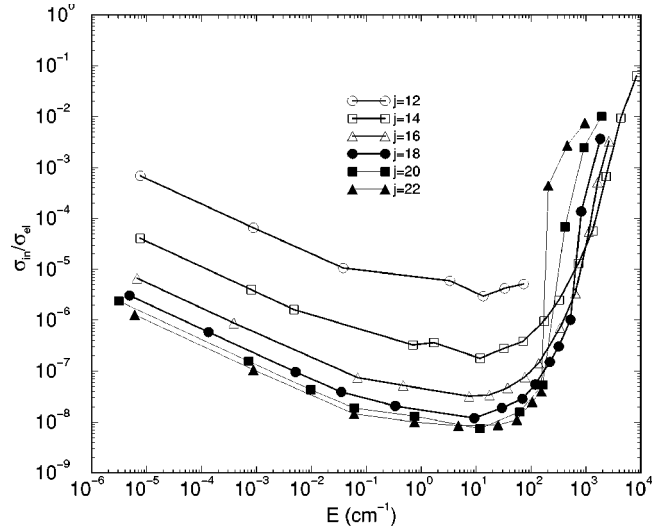

FIG. 4. Ratio of inelastic to elastic cross section as a function of translational energy for collisions of ^{3}He with $H_2(v=0,j)$. The inelastic cross section includes contributions from all possible deexcitation channels.

[8] that the dimensionless ratio β_{vj}/α_{vj} is not very sensitive to the details of the potential-energy surface when the last bound state of the van der Waals complex is not too close to zero.

III. RESULTS

Figure 4 shows the ratio of inelastic to elastic cross section as a function of kinetic energy for collisions of ^{3}He with $H_2(v=0,j)$. The inelastic cross section includes contributions from all possible deexcitation channels, and is greatly reduced when the quasiresonant $\Delta v=1,\Delta j=-2$ transition becomes energetically disallowed. This occurs for translational energies in the range 100–1000 cm^{-1}. When the temperature is below this energy range, the rotationally hot molecules are significantly more stable against collisional relaxation. The curves shown in Fig. 4, which are consistent with those reported previously [6], demonstrate that the $v=0$ states of the molecule allow a wider range of rotational levels to be stable against collision (e.g., the $v=2$ states allowed only the $j=22$ level to be stable against collision [6]). For $j\geqslant 24$, the $\Delta v=1,\Delta j=-2$ transition is energetically allowed as the translational energy is reduced to zero. Therefore, the total inelastic cross section is quite large for $j\geqslant 24$, and the ratio σ_{in}/σ_{el} does not give the steplike behavior shown in the figure. The sharpness of the step is greatest for $j=22$ and decreases with decreasing j. The energy where the step is located and the magnitude of the ratio σ_{in}/σ_{el} increases with decreasing j. Wigner threshold behavior occurs for energies below 10^{-2} cm^{-1}.

Figure 5 shows total quenching rate coefficients for collisions of He with $H_2(v=0,j)$ in the limit of zero temperature. The rate coefficients, which include contributions from all possible deexcitation channels, decrease smoothly with j with two obvious exceptions. When $j\geqslant 12$, the $\Delta v=1,\Delta j=-4$ transition is energetically allowed and we see a sudden increase in the total quenching rate coefficient for $j=12$. Likewise, when $j\geqslant 24$, the $\Delta v=1,\Delta j=-2$ transition is energetically allowed and we see a sudden increase in the total quenching rate coefficient for $j=24$. The qualitative behavior of the rate coefficients is identical for both isotopes of the helium collision partner. The magnitude of the curve is generally controlled by the location of the most weakly bound state of the three-body complex.

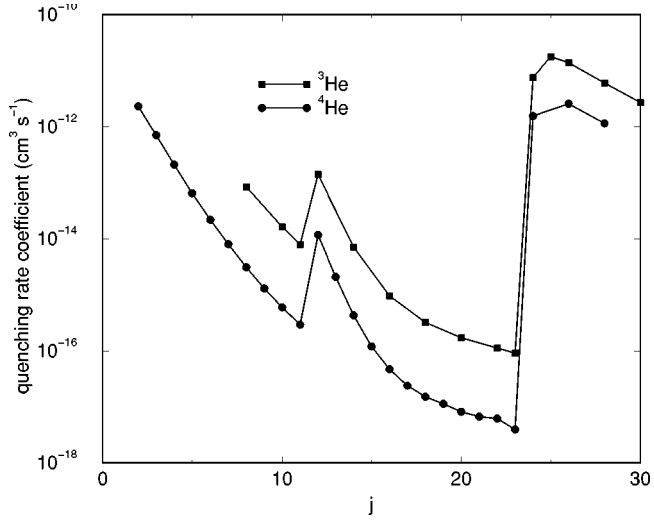

FIG. 5. Quenching rate coefficients for collisions of He with $H_2(v=0,j)$ in the limit of zero temperature. The rate coefficients include contributions from all possible deexcitation channels.

Figure 6 shows the total quenching rate coefficients for collisions of ^{4}He with $H_2(v,j)$ in the limit of zero temperature. The rate coefficients, which include contributions from all possible deexcitation channels, reveal a characteristic curve for $v>0$ that is different from the $v=0$ curve of Fig. 5. The reason is the availability of $\Delta v=-1$ quasiresonant transitions. Like the $v=0$ case, it is the pure rotational transitions that dominate the quenching for $j<7$. However,

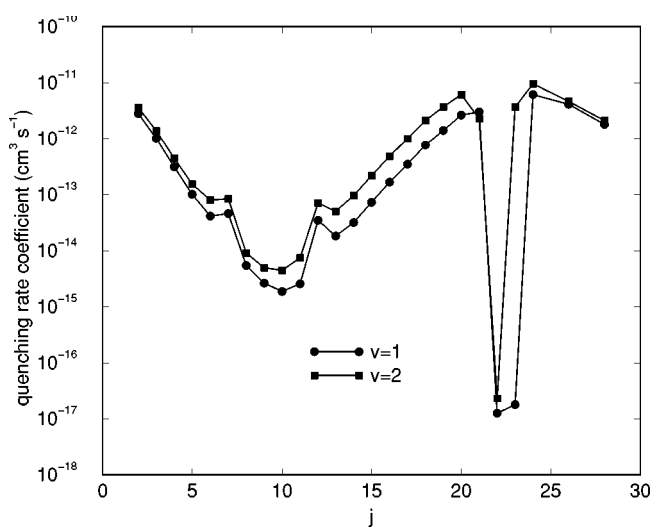

FIG. 6. Quenching rate coefficients for collisions of ^{4}He with $H_2(v,j)$ in the limit of zero temperature. The rate coefficients include contributions from all possible deexcitation channels.

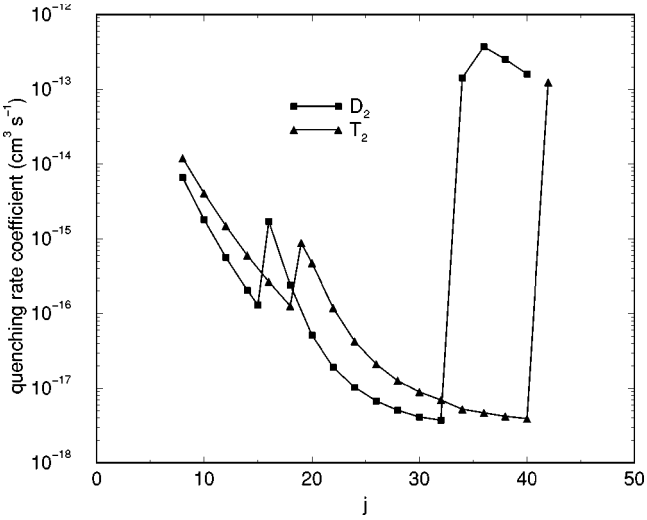

FIG. 7. Quenching rate coefficients for collisions of ^{3}He with $D_2(v=0,j)$ and $T_2(v=0,j)$ in the limit of zero temperature. The rate coefficients include contributions from all possible deexcitation channels.

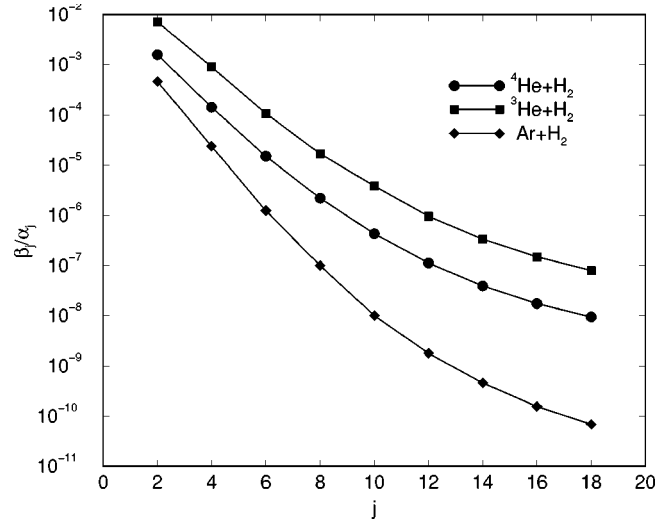

FIG. 8. Ratio of imaginary to real part of the complex scattering length as a function of rotational level. The imaginary part β_j includes only contributions from pure rotational deexcitation channels.

when $j=7$ there is a strong contribution from the $\Delta v=-1,\Delta j=4$ transition and there is an upturn in the curves. For $j>7$, the $\Delta v=-1,\Delta j=4$ transition is not energetically allowed and there is a sharp downturn in the curves. When $j\geqslant 12$, the $\Delta v=1,\Delta j=-4$ transition is energetically allowed as in the $v=0$ case, and we see a sudden increase in the total quenching rate coefficient for $j=12$. Unlike the $v=0$ case, however, there is a smooth increase in the rate coefficient for $13\leqslant j\leqslant 20$. This is due to the dominant $\Delta v=-1,\Delta j=2$ quasiresonant transition. When $j=22$ there is a sharp decrease in the total quenching rate coefficient due to the closing of the $\Delta v=-1,\Delta j=2$ quasiresonant transition. When $j\geqslant 24$ (23 for $v=2$), the $\Delta v=1,\Delta j=-2$ transition is energetically allowed as in the $v=0$ case, and we see a sharp increase in the total quenching rate coefficient.

Figure 7 shows quenching rate coefficients for collisions of ^{3}He with $D_2(v=0,j)$ and $T_2(v=0,j)$ in the limit of zero temperature. The characteristic behavior is the same as in Fig. 5 for $H_2(v=0,j)$. As the moment of inertia is increased, the rotational energy spacing decreases and the onset for the opening of quasiresonant transitions is pushed out to higher values of j. The opening of the $\Delta v=1,\Delta j=-4$ transition occurs at $j=16$ for $D_2(v=0,j)$ and at $j=19$ for $T_2(v=0,j)$, whereas the opening of the $\Delta v=1,\Delta j=-2$ transition occurs at $j=34$ for $D_2(v=0,j)$ and at $j=42$ for $T_2(v=0,j)$. Because pure rotational quenching decreases exponentially with increasing j, the states that are most stable against collisional relaxation will be those states whose j value is the largest possible value such that $\Delta j=-2\Delta v$ transitions are closed. This occurs at $j=32$ and $j=40$, respectively, for D_2 and T_2. The quantitative results for D_2 and T_2 demonstrate that the QRVR effect does not have a strong dependence on the moment of inertia of the molecule. Instead the $j_{QR}^{(n)}$ and j_D values simply increase and the characteristic behavior is not affected. This is in contrast to previous speculations that the effect would be most pronounced for light systems [6,7]. Of course, if the moment of inertia is large enough that $j_{QR}^{(n)}>j_D$, then the nth-order QRVR effect may be absent. Also, the moment arm influences the rotational anisotropy of the interaction. The long-range anisotropy in the potential-energy surface may be estimated using the relation [30]

$$V_L(R,\gamma)\approx -\frac{C_6}{R^6}\left[1+\frac{\alpha_\parallel-\alpha_\perp}{\alpha_\parallel+2\alpha_\perp}P_2(\cos\gamma)\right], \qquad (11)$$

where $\alpha_\parallel$ and $\alpha_\perp$ are the respective components of the diatomic polarizability that are parallel and perpendicular to the internuclear axis. If the moment arm is small, as in the case of H_2, then the rotational anisotropy $\alpha_\parallel-\alpha_\perp$ tends to be small and the pure rotational quenching is less efficient.

As discussed in Sec. II, the numerical values of the cross sections and rate coefficients are very sensitive to the details of the potential-energy surface. Because potential-energy surfaces are not designed for ultracold collisions, it is useful to present results of paramaters that are not as sensitive to the details of the surface. The ratio β/α is one such parameter. Figures 8–11 show results for this parameter as a function of rotational level and energy gap for several systems. In Figs. 8 and 9, the imaginary component includes only contributions from pure rotational deexcitation. The curves are very smooth and the exponential decay with energy gap is clearly seen in Fig. 9. In Fig. 10, the ratio β/α is given as a function of j for ^{4}He collisions with H_2 in the $v=0$ and $v=2$ states. The rovibrational transitions are included in the calculations and β_{vj} contains contributions from all possible deexcitation channels. A comparison of Fig. 8 and Fig. 10 demonstrates that the structure in the curves is a consequence of allowed and forbidden QRVR transitions. The real part of the scattering length varies slowly so the characteristic behavior of β/α is similar to the total quenching rate coefficients shown in Figs. 5 and 6.

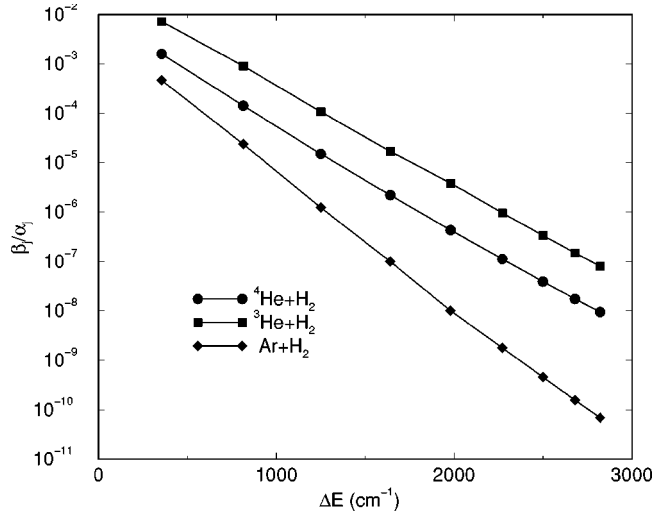

FIG. 9. Ratio of imaginary to real part of the complex scattering length as a function of the energy gap between initial and final diatomic states. The imaginary part β_j includes only contributions from pure rotational deexcitation channels.

Figure 11 includes results for H_2+H_2 and $He+O_2$ collisions. The $He+O_2$ calculations were performed using the potential-energy surface of Groenenboom and Struniewicz [23]. A full account of the calculations, which agree with those reported by Balakrishnan and Dalgarno for low rotational levels [24], will be given elsewhere. The H_2+H_2 calculations were performed within the rigid-rotor approximation [25] using the interaction potential of Zarur and Rabitz [26]. The $He+H_2$ and $Ar+H_2$ results were obtained using the potential-energy surfaces of Muchnick and Russek [27] and Schwenke, Walch and Taylor [28], respectively. The results for $He+O_2$ show that the decrease in relaxation efficiency with increasing j is extremely slow. Although it was not possible to obtain converged results for $j>40$, the trend

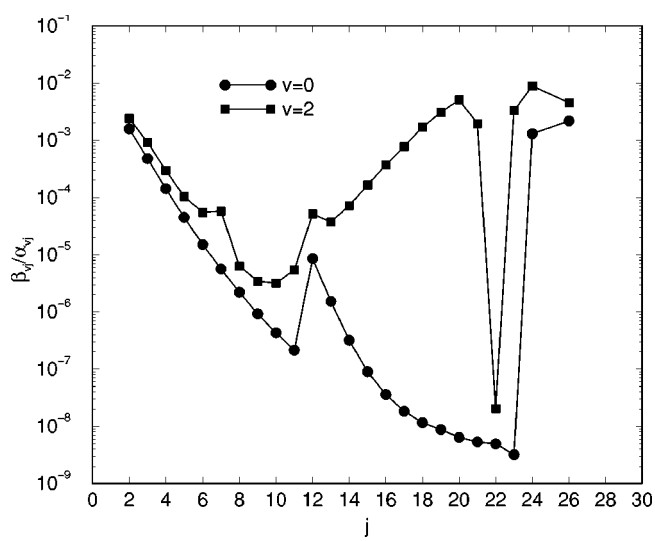

FIG. 10. Ratio of imaginary to real part of the complex scattering length as a function of rotational level for collisions of ^{4}He with $H_2(v,j)$ in the limit of zero temperature. The imaginary part β_{vj} includes contributions from all possible deexcitation channels.

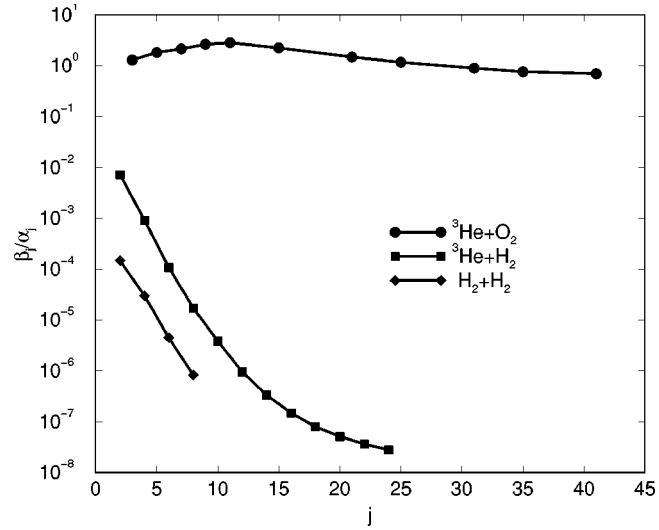

FIG. 11. Ratio of imaginary to real part of the complex scattering length as a function of rotational level. The imaginary part β_j includes only contributions from pure rotational deexcitation channels.

in the data suggests that the quenching will remain too great for any rotational level to be a viable candidate for cooling and trapping.

IV. CONCLUSION

We have performed detailed quantum-mechanical calculations for cold collisions of helium atoms with hydrogen, deuterium, and tritium molecules. The rotational distributions of the total quenching rate coefficients show a characteristic behavior that is independent of the rotational inertia of the molecule. The QR and dissociation rotational levels both increase with increasing inertia, but the characteristic behavior of the distributions is unaffected. From these observations we may draw general conclusions about other diatomic systems from the knowledge of the term energies. If $j_{QR}^{(2)}$ is less than j_D for a given vibrational level, then the zero-temperature collisional quenching may be greatly suppressed for $j=j_{QR}^{(2)}$. Many molecules have a value for $j_{QR}^{(2)}$ that is greater than j_D. In this case, the $v=0$ rate coefficients may still be significantly suppressed for $j\approx j_D$, but there cannot be any bound rotationally *and vibrationally* excited molecules that are stable against collision.

Highly rotationally excited molecules may be produced over a distribution of rotational levels using an optical centrifuge [3] or in a single state selected rotational level using the experimental scheme proposed by Stwalley and coworkers [2]. It may also be possible to use the collisional properties to produce molecules in a single rotational level for states with $v>0$ (e.g., see the $v=2$ curve of Fig. 6). In any experimental scheme, the key to producing rotationally hot molecules that are stable against collision is to cool the molecules to temperatures where translational energy cannot be used to facilitate a QRVR transition.

The optical centrifuge allows the use of a cold gas as a starting point for the excitation. Cooling and trapping tech-

niques that rely on elastic collisions could then be used to further reduce the translational temperature of specific states of the molecule [6]. Because specific rotationally hot molecules are stable against cold collisions, it may be possible to use a gas of such molecules as a means of storing energy. If the density of the gas is not too large, then the molecules would decay primarily through quadrapole radiation. In the case of H_2 the lifetime for quadrapole decay when $18<j<22$ is typically 3–4 days [29]. The rate coefficients for He-H_2 and H_2-H_2 collisions suggest that it may be possible to maintain a large density of molecules for these values of j before ultimately losing them to collisional or radiative decay.

We have also performed calculations for helium collisions with highly rotationally excited oxygen molecules. The rotational anisotropy of the He-O_2 potential-energy surface is large enough that the pure rotational quenching is very efficient at all values of j that were studied. Generally, strong rotational anisotropy will limit the possibilities for cooling and trapping. The results reported in this work suggest that hydrogen molecules would offer the greatest stability against collisional relaxation. However, they would also be the most difficult to rotate because the magnitude of $\alpha_{\parallel}-\alpha_{\perp}$ is what allows the diatomic molecules to be spun to such high rotational levels [1]. In a practical application, it may be desireable to sacrifice some collisional stability in order to gain other advantages. For example, a molecule with a magnetic dipole moment would allow a convenient trapping scheme [10]. If the molecule retains enough collisional stability and allows enough state selectivity (e.g., the $v=2$, $j=22$ state of hydrogen), then it is conceivable that evaporative cooling could be used in an effort to reach Bose-Einstein condensation.

ACKNOWLEDGMENT

This work was funded by the National Science Foundation Grant No. PHY-0070920.

[1] J. Karczmarek, J. Wright, P. Corkum, and M. Ivanov, Phys. Rev. Lett. **82**, 3420 (1999).

[2] J. Li, J.T. Bahns, and W.C. Stwalley, J. Chem. Phys. **112**, 6255 (2000).

[3] D.M. Villeneuve, S.A. Aseyev, P. Dietrich, M. Spanner, M.Y. Ivanov, and P.B. Corkum, Phys. Rev. Lett. **85**, 542 (2000).

[4] R.C. Forrey, N. Balakrishnan, A. Dalgarno, M. Haggerty, and E.J. Heller, Phys. Rev. Lett. **82**, 2657 (1999).

[5] R.C. Forrey, N. Balakrishnan, A. Dalgarno, M. Haggerty, and E.J. Heller, Phys. Rev. A **64**, 022706 (2001).

[6] R.C. Forrey, Phys. Rev. A **63**, 051403 (2001).

[7] A.J. McCaffery, J. Chem. Phys. **113**, 10 947 (2000).

[8] J.C. Flasher and R.C. Forrey, Phys. Rev. A **65**, 032710 (2002).

[9] B. Stewart, P.D. Magill, T.P. Scott, J. Derouard, and D.E. Pritchard, Phys. Rev. Lett. **60**, 282 (1988); T.P. Scott, N. Smith, P.D. Magill, D.E. Pritchard, and B. Stewart, J. Phys. Chem. **100**, 7981 (1996).

[10] J.D. Weinstein, R. deCarvalho, T. Guillet, B. Friedrich, and J.M. Doyle, Nature (London) **395**, 148 (1998); J. Doyle and B. Friedrich, Chem. Br. **35**, 31 (1999).

[11] F. Stienkemeier, W.E. Ernst, J. Higgins, and G. Scoles, J. Chem. Phys. **102**, 615 (1995); J. Higgins, C. Callegari, J. Reho, F. Stienkemeier, W.E. Ernst, K.K. Lehmann, M. Gutowski, and G. Scoles, Science **273**, 629 (1996).

[12] T.A. Brunner and D.E. Pritchard, Adv. Chem. Phys. **50**, 589 (1982).

[13] A.J. McCaffery, Z.T. Alwahabi, M.A. Osborne, and C.J. Williams, J. Chem. Phys. **98**, 4586 (1992).

[14] P.D. Magill, B. Stewart, N. Smith, and D.E. Pritchard, Phys. Rev. Lett. **60**, 1943 (1988).

[15] W.J. Hovingh and R. Parson, Chem. Phys. Lett. **158**, 222 (1989).

[16] S. Clare and A.J. McCaffery, J. Phys. B **33**, 1121 (2000).

[17] D.W. Schwenke, J. Chem. Phys. **89**, 2076 (1988).

[18] W.T. Zemke and W.C. Stwalley, J. Phys. Chem. **97**, 2053 (1993).

[19] R.S. Friedman, J. Quant. Spectrosc. Radiat. Transf. **43**, 225 (1990).

[20] J.F. Babb and A. Dalgarno, Phys. Rev. A **51**, 3021 (1995).

[21] This point was brought to my attention by W. C. Stwalley.

[22] J.M. Hutson and S. Green, MOLSCAT computer code, version 14 (1994), distributed by Collaborative Computational Project No. 6 of the Engineering and Physical Sciences Research Council (UK).

[23] Groenenboom and Struniewicz, J. Chem. Phys. **113**, 9562 (2000).

[24] N. Balakrishnan and A. Dalgarno, J. Phys. Chem. **105**, 2348 (2001).

[25] S. Green, J. Chem. Phys. **62**, 2271 (1975).

[26] G. Zarur and H. Rabitz, J. Chem. Phys. **60**, 2057 (1974).

[27] P. Muchnick and A. Russek, J. Chem. Phys. **100**, 4336 (1994).

[28] D.W. Schwenke, S.P. Walch, and P.R. Taylor, J. Chem. Phys. **98**, 4738 (1993).

[29] L. Wolniewicz, I. Simbotin, and A. Dalgarno, Astrophys. J., Suppl. Ser. **115**, 293 (1998).

[30] A.D. Buckingham, Adv. Chem. Phys. **12**, 107 (1967).